Lithium niobate nanowires synthesis, optical properties, and manipulation

Rachel Grange,[1,a)] Jae-Woo Choi,[1,2] Chia-Lung Hsieh,[1,2] Ye Pu,[1,2] Arnaud Magrez,[3] Rita Smajda,[3] László Forró,[3] and Demetri Psaltis[1,2]
[1]*École Polytechnique Fédérale de Lausanne (EPFL), School of Engineering, Optics Laboratory, 1015 Lausanne, Switzerland*
[2]*Department of Electrical Engineering, California Institute of Technology, Pasadena, California 91125, USA*
[3]*École Polytechnique Fédérale de Lausanne (EPFL), Institute of Physics of Condensed Matter (IPMC), Laboratoire des Nanostructures et Nouveaux Matériaux Electroniques (LNNME), 1015 Lausanne, Switzerland*

(Received 20 July 2009; accepted 31 August 2009; published online 6 October 2009)

Free-standing lithium niobate nanowires ($LiNbO_3$) are synthesized by the hydrothermal route. The polarization response of the second harmonic generation (SHG) signal is measured in a single nanowire and used to identify the crystal orientation by matching with bulk $LiNbO_3$ nonlinear optical susceptibility. The electrical manipulation of a $LiNbO_3$ nanowire and its monitoring through the SHG signal in a fluidic setup are demonstrated. © *2009 American Institute of Physics*. [doi:10.1063/1.3236777]

Lithium niobate ($LiNbO_3$) is one of the most versatile optical and electronic materials, being simultaneously nonlinear-optic, electro-optic, acousto-optic, ferroelectric, piezoelectric, and photorefractive. Since the discovery of its ferroelectricity,[1] $LiNbO_3$ has seen constantly growing engineering applications, for instance, in the telecom industry for frequency conversion and electro-optic modulation.[2] In the past decade, significant interest has been focused on the synthesis of nanoscale materials due to their interesting properties emerging from the dimensional confinement, which has great potential applications in devices. Indeed, one-dimensional nanosized $LiNbO_3$ crystals open up large perspectives for this widely used material.

Many synthesis routes are being developed for $LiNbO_3$ at the nanoscale resulting in different size, shape, and crystalline quality. $LiNbO_3$ nanoparticles have been previously produced by milling,[3] nonaqueous route,[4] sol-gel method,[5] or hydrothermal route.[6] Arrays of polycrystalline $LiNbO_3$ nanotubes have also been reported,[7] as well as a solution-phase synthesis to produce rodlike structures among other multiple structures.[8] Here we report the hydrothermal growth of free-standing $LiNbO_3$ nanowires and their characterization. We study the second harmonic generation (SHG) properties of these $LiNbO_3$ nanowires and show that nanowires are efficient nanoscale second harmonic light source. The SHG study also reveals the orientation of the crystal structure, paving the way for future applications of the unique crystal properties of $LiNbO_3$ nanowires. As one particular example, we demonstrate the manipulation of the nonlinear optical response of a single nanowire using external electric fields in microfluidic channels, while monitoring its SHG signal simultaneously. Indeed, $LiNbO_3$ nanowires can be used as imaging probes,[9] as nanoscale electro-optical devices such as localized photon sources, or as components of nanomachines.

The $LiNbO_3$ nanowires were synthesized using the hydrothermal route at low temperatures, similar to the synthesis of $KNbO_3$ nanowires.[10] Niobium pentoxide (Nb_2O_5) powder is added to distilled water in which lithium hydroxide powder is dissolved. The mixture (in a Teflon vessel) is heated in an autoclave at about 150 °C and under pressure (approximately 5 bars), producing a precipitate. The solid precipitate is filtered, washed with water and ethanol, and dried at 120 °C. The x-ray diffraction pattern of the synthesized $LiNbO_3$ powder correlates with the peak positions of standard bulk $LiNbO_3$ (Fig. 1). Within the precipitate, nanowires are present as well as nanoparticles (Fig. 1 inset). The scanning electron microscope (SEM) pictures show typical aggregates of nanowires up to 3-μm-long and around 50 nm in diameter, as well as $LiNbO_3$ nanoparticles with diameters of 20–30 nm. The fact that free-standing nanowires are observed, as in the inset of Fig. 2, is probably due to the low solubility of Nb_2O_5 in the liquid phase, which is instantaneously used to form $LiNbO_3$.[11] The nanowires can be separated from the nanoparticles through simple centrifugation.

To perform correlated SEM and SHG studies, we first dilute the $LiNbO_3$ precipitate into methanol and deposit a droplet of the colloidal solution on an indium tin oxide (ITO)-coated glass substrate for SEM imaging. Using a SEM image (Fig. 2 inset), we locate a single wire and measure its diameter (50 nm) and length (700 nm). The same nanowire is then located again for SHG investigation under a white light

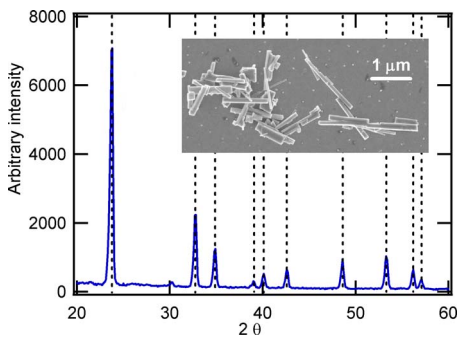

FIG. 1. (Color online) X-ray diffraction pattern of $LiNbO_3$ synthesized nanopowder. The dashed lines indicate the location of standard bulk $LiNbO_3$ peaks. Inset: SEM images of the $LiNbO_3$ synthesized powder containing nanowires as well as nanoparticles.

a)Electronic mail: rachel.grange@epfl.ch.

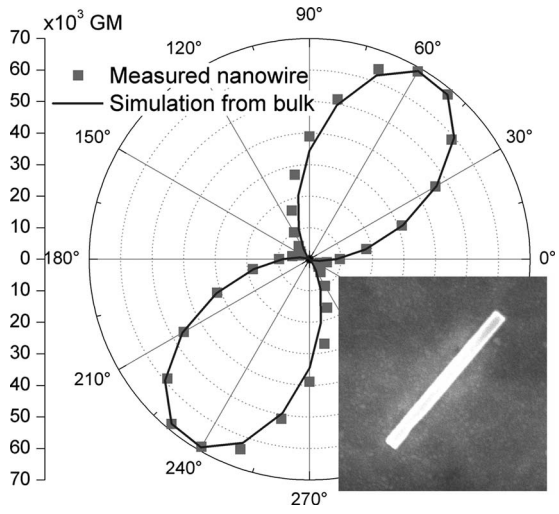

FIG. 2. The polarization response of the SHG from a single $LiNbO_3$ nanowire in polar coordinate (1 GM=10^{-50} cm^4 s $photon^{-1}$). Inset: SEM of the single free-standing $LiNbO_3$ nanowire deposited on ITO-coated glass used for the polarization measurement. Nanowire dimensions: 50-nm-wide and 700-nm-long.

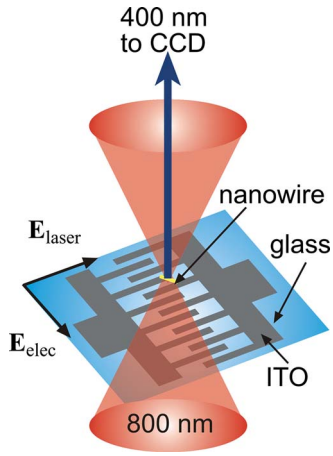

FIG. 3. (Color online) Schematic of the setup for the electrical and optical manipulation. Two torques attempt to orient the nanowire: the electric field due to the polarization of the 800 nm laser (E_{laser}) and the external applied electric field (E_{elec}).

transmission microscope using prescribed markers on the ITO glass slide.

In the SHG study, a laser beam from a Ti:sapphire oscillator operated at 800 nm wavelength, with 150 fs pulse and 76 MHz repetition rate, is focused down to 20 μm diameter on the sample at an average power of 160 mW. The SHG signal at 400 nm is then collected with an oil immersion microscope objective (100×, NA 1.4) and recorded on an electron multiplying charge coupled device after filtering out the fundamental pump wavelength. The polarization of the pump beam is rotated with a half-wave plate to obtain polarization-dependent SHG response. Figure 2 shows the polarization-dependent response of the SHG emission for the single $LiNbO_3$ nanowire (Fig. 2 inset). At different incident polarization angles, the SHG intensities are recorded. The measurements of SHG emission are plotted in terms of SHG scattering cross-section $\sigma_{2\omega}=W_{2\omega}/(I_\omega)^2$ in the entire 4π solid angle, where $W_{2\omega}$ is the total emission power at 2ω (400 nm) and I_ω is the excitation intensity at ω (800 nm). We use Goeppert–Mayer (GM) unit for SHG scattering cross-section (1 GM=10^{-50} cm^4 s $photon^{-1}$).

In the hydrothermal process, the growth orientation may not be precisely known, as is the case for single crystalline $KNbO_3$ nanowires, since there is no preferential growth orientation. Several single crystalline nanowires were found with different crystallographic directions following the long axis of the wires.[12] From the SHG response, however, the crystal orientation of the nanowire can be determined based on the second-order nonlinear susceptibility tensor and, in our case, we will show that the *c*-axis is along the long axis of the wire. This is possible because the precise relationship between the pump polarization angle and the nanowire layout can be obtained through the SEM picture (inset of Fig. 2). The SHG response of the nanowire is highly polarization-sensitive, with the maximum intensity reached when the pump polarization is parallel to the long axis of the wire. In order to find the crystal orientation, we calculate the theoretical SHG response for every possible orientation in 1° steps and match the response pattern with the measurement. The orientation that produces the best match is then chosen to be the crystal orientation. In our theoretical model, we take into account that the large length-diameter ratio of the nanowire induces a change to the internal electric field component that is perpendicular to the wire but no modification to the component that is parallel to it.[13] The measured SHG response matches the fit parameters corresponding to a *c*-axis parallel to the nanowire long axis. At the optimal excitation polarization, the SHG cross-section of the nanowire is 69 $\times 10^3$ GM. The SHG response of the nanowire can be well fitted with our model using nonlinear susceptibilities of bulk $LiNbO_3$. In our model, we neglected the contributions from the surface, which are significant only in centrosymmetric materials.[14,15] Note that the size of the nanowire is not much smaller than the wavelength and it cannot be considered to be in the pure Rayleigh regime. Interferences may occur within the SHG radiation from the nanowire introducing a difference of intensity response between the measured nanowire and the model. Indeed, the measured intensity is 8.7 times weaker than expected by the model, but the shape perfectly fits the results.

As a potential application of the unique SHG property of $LiNbO_3$ nanowires, we demonstrate the electrical manipulation of the SHG signal in a fluidic setup. We manipulate the orientation of an optically trapped $LiNbO_3$ nanowire in a fluidic environment using an externally applied electric field and monitor its SHG response. As illustrated in Fig. 3, the optical tweezers is constructed using a femtosecond Ti:sapphire laser operated at 800 nm wavelength. The nanowire under investigation is suspended in an aqueous fluid supported on a glass substrate that is patterned with ITO electrodes.[16] The focus of the tweezers beam is located between the two electrodes and slightly outside the fluid region so that the nanowire is pressed on the substrate and is oriented orthogonal to the beam propagation. Figure 4 shows white light images [Figs. 4(a) and 4(c)] and SHG signals [Figs. 4(b) and 4(d)] of the nanowire suspended in deionized water. When no external electric field (E=0 V_{pp}) is applied [Figs. 4(a) and 4(b)] the nanowire is oriented along the electrode within the plane of the substrate following the polarization of the tweezers beam only. When an external electric field (E=10 V_{pp}) is applied to the nanowire using the electrodes [Fig. 4(c) and 4(d)], an additional electro-orientation force results due to the dielectrophoretic (DEP)

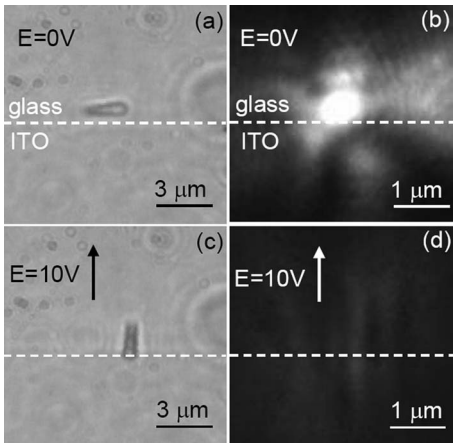

FIG. 4. DEP response of a $LiNbO_3$ nanowire suspended in 170 μS/cm conductivity de-ionized water [(a) and (b)] without and [(c) and (d)] with an electric field of 10 V_{pp} at 150 kHz. (a) and (c) White light images; (b) and (d) SHG response (enhanced online). [URL: http://dx.doi.org/10.1063/1.3236777.1] [URL: http://dx.doi.org/10.1063/1.3236777.2]

response of the $LiNbO_3$ nanowire. The torque on the nanowire due to the external electric field (10^6 V/m) is more than ten times greater in magnitude than the torque on the nanowire due to the optical polarization of the laser for 3 mW power and 10 μm beam radius at the sample position (10^5 V/m). Under this 10 V_{pp} electric field with a frequency of 150 kHz in a fluid of 170 μS/cm conductivity, the $LiNbO_3$ nanowire is aligned with the field due to positive DEP forces. Note that the orientation of the nanowire in the external electric field is mostly influenced by its shape and not by the different permittivities of $LiNbO_3$.

Due to the polarization dependency of the wire, the second harmonic signal is strongly attenuated in Fig. 4(d) compared to Fig. 4(b) allowing for monitoring the position of the wire. Increasing the conductivity of the suspension as well as changing the frequency of the applied electric field can change the type of DEP force on the nanowire, which will result in the nanowire being not aligned with the field.[17] We notice the crossover between negative and positive DEP when the conductivity of the solution is around 170 μS/cm.

DEP forces have already been used to orient and manipulate several different types of dielectric nanowires.[18] In our case, besides the external applied field for DEP, the use of the 800 nm laser brings two advantages: maintaining the nanowire in a certain position with the trapping property and generating the second harmonic signal that helps locate the nanowire, especially when the particle is subwavelength in size and cannot be optically resolved. The combination of the applied external electric field and the polarization of the laser beam are useful for several applications. First, a rough estimate of the conductivity near the nanowire may be obtained, for example, if there is a conductivity gradient in the sample.[19] Second, a capability to determine the hydrodynamic conditions is possible within a fluidic environment.[20] The SHG from these nanowires allow for high signal-to-noise response and interferometric detection for subwavelength size structures due to the coherence of the SHG process. Third, the electrical manipulation makes the integration of several of these nanowires possible to create massively parallel devices.[21] Optical means would be used to probe individual nanowires and electrical means to manipulate several of the nanowires at once.

In conclusion, we have grown free-standing, well-formed $LiNbO_3$ nanowires through the hydrothermal route at low temperature. The optical characterization of the second harmonic response of a single nanowire could be matched with bulk $LiNbO_3$ nonlinear optical susceptibility. As bulk $LiNbO_3$, nanowires show a strong SHG response. According to the simulation, the *c*-axis of the crystal is parallel to the long axis of this particular nanowire. Then, we applied an external electric field to change the DEP response of the nanowire and, simultaneously, we trapped single nanowires in an 800 nm laser beam. The rotation of the second harmonic signal was monitored and strong attenuation was shown that could be used in the future to detect signal of objects below the diffraction limit of an optical system. Moreover, we expect $LiNbO_3$ nanowires to possess other similar properties as bulk material such as photovoltaic effect that will be further studied.

At the Optics Laboratory, this project is partly supported by the NCCR Quantum Photonics program of the Swiss National Foundation. Work at the LNNME was carried out within the NCCR Nanoscience program of the Swiss National Foundation.

[1] B. T. Matthias and J. P. Remeika, Phys. Rev. **76**, 1886 (1949).
[2] E. L. Wooten, K. M. Kissa, A. Yi-Yan, E. J. Murphy, D. A. Lafaw, P. F. Hallemeier, D. Maack, D. V. Attanasio, D. J. Fritz, G. J. McBrien, and D. E. Bossi, IEEE J. Sel. Top. Quantum Electron. **6**, 69 (2000).
[3] J. R. Schwesyg, H. A. Eggert, K. Buse, E. Sliwinska, S. Khalil, M. Kaiser, and K. Meerholz, Appl. Phys. B: Lasers Opt. **89**, 15 (2007).
[4] M. Niederberger, N. Pinna, J. Polleux, and M. Antonietti, Angew. Chem., Int. Ed. **43**, 2270 (2004).
[5] L. H. Wang, D. R. Yuan, X. L. Duan, X. Q. Wang, and F. P. Yu, Cryst. Res. Technol. **42**, 321 (2007).
[6] C. H. An, K. B. Tang, C. R. Wang, G. Z. Shen, Y. Jin, and Y. T. Qian, Mater. Res. Bull. **37**, 1791 (2002).
[7] L. L. Zhao, M. Steinhart, M. Yosef, S. K. Lee, and S. Schlecht, Sens. Actuators B **109**, 86 (2005).
[8] B. D. Wood, V. Mocanu, and B. D. Gates, Adv. Mater. **20**, 4552 (2008).
[9] C.-L. Hsieh, R. Grange, Y. Pu, and D. Psaltis, Opt. Express **17**, 2880 (2009).
[10] A. Magrez, E. Vasco, J. W. Seo, C. Dieker, N. Setter, and L. Forro, J. Phys. Chem. B **110**, 58 (2006).
[11] E. Vasco, A. Magrez, L. Forro, and N. Setter, J. Phys. Chem. B **109**, 14331 (2005).
[12] G. K. L. Goh, C. G. Levi, J. H. Choi, and F. F. Lange, J. Cryst. Growth **286**, 457 (2006).
[13] J. Wang, M. S. Gudiksen, X. Duan, Y. Cui, and C. M. Lieber, Science **293**, 1455 (2001).
[14] J. I. Dadap, J. Shan, K. B. Eisenthal, and T. F. Heinz, Phys. Rev. Lett. **83**, 4045 (1999).
[15] V. Barzda, R. Cisek, T. L. Spencer, U. Philipose, H. E. Ruda, and A. Shik, Appl. Phys. Lett. **92**, 113111 (2008).
[16] J. W. Choi, A. Pu, and D. Psaltis, Opt. Express **14**, 9780 (2006).
[17] N. G. Green and H. Morgan, J. Phys. D: Appl. Phys. **30**, L41 (1997).
[18] P. J. Burke, in *Encyclopedia of Nanoscience and Nanotechnology*, edited by H. S. Nalwa (American Scientific, Stevenson Ranch, 2004), Vol. 6, p. 623.
[19] G. H. Markx, P. A. Dyda, and R. Pethig, J. Biotechnol. **51**, 175 (1996).
[20] K. Keshoju, H. Xing, and L. Sun, Appl. Phys. Lett. **91**, 123114 (2007).
[21] M. W. Li, R. B. Bhiladvala, T. J. Morrow, J. A. Sioss, K. K. Lew, J. M. Redwing, C. D. Keating, and T. S. Mayer, Nat. Nanotechnol. **3**, 88 (2008).